Investigating the Modulation of Spatio-Temporal and Oscillatory Power Dynamics by Perceptible and Non-perceptible Rhythmic Light Stimulation

Katharina Lingelbach[1,2(✉)], Isabel Schöllhorn[3], Alexander M. Dreyer[2], Frederik Diederichs[1], Michael Bui[1], Michael Weng[4], Jochem W. Rieger[2], Ina Petermann-Stock[4], and Mathias Vukelić[1]

[1] Fraunhofer Institute for Industrial Engineering IAO, Nobelstr. 12, Stuttgart, Germany
{katharina.lingelbach,frederik.diederich,michael.bui,
mathias.vukelic}@iao.fraunhofer.de
[2] Department of Psychology, Carl von Ossietzky University, Oldenburg, Germany
{alexander.dreyer,jochem.rieger}@uni-oldenburg.de
[3] Centre for Chronobiology, Psychiatric Hospital of the University of Basel, Basel, Switzerland
isabel.schoellhorn@upk.ch
[4] Volkswagen Group Innovation, Wolfsburg, Germany
{michael.weng,ina.petermann-stock}@volkswagen.de

Abstract. Several studies emphasize the great potential of rhythmic light stimulation to evoke steady-state visual evoked potentials (SSVEPs) measured via electroencephalographic (EEG) recordings as a safe method to modulate brain activity. In the current study, we investigated visual event-related potentials (ERPs) and oscillatory power evoked by perceptible (above a previously estimated individual threshold) and non-perceptible (below the individual threshold) frequency-modulated rhythmic light stimulation at 10 Hz via a light-emitting diode. Furthermore, we examined the effect of overt and covert attention by asking participants to (1) directly focus on the light source (overt attention condition) and (2) indirectly attend it (covert attention condition). Our results revealed entrainment effects reflected in both ERPs and oscillatory power in the EEG even for a stimulation intensity below the individual perceptibility threshold and without directly fixating the light source. This non-invasive stimulation method shows strong potential for naturalistic non-clinical applications.

Keywords: Neuroergonomics · Electroencephalography · Oscillatory power · Event-related potentials · Non-perceptible and perceptible stimulation · Attention · Steady-state visual evoked potentials

1 Introduction

In the last decades, the phenomenon of synchronized neuronal firing, so-called steady-state visual evoked potentials (SSVEPs; e.g., [1]), evoked by rhythmic light stimulation

H. Ayaz et al. (Eds.): AHFE 2021, LNNS 259, pp. 11–19, 2021.
https://doi.org/10.1007/978-3-030-80285-1_2

has been intensively researched. SSVEPs are neurophysiological responses that can be measured via the electroencephalography (EEG) and are well suited for brain computer interface (BCI) applications due to their high signal-to-noise ratio (SNR) [2, 3]. Moreover, such rhythmic light stimulations are suggested to be a safe method to modulate brain activity and seem to have effects comparable to other non-invasive brain stimulation [4, 5]. Especially, frequency-modulated (FM) stimulations are promising protocols allowing for less perceptible visual stimulation and, thus, decrease of potential eye fatigue and user discomfort [6–8]. During a FM stimulation, the carrier frequency (usually a high frequency, e.g., 40 Hz) is modulated by a second frequency (i.e., the modulation frequency, e.g., 30 Hz) and SSVEPs are evoked at the frequency of the difference (40–30 = 10 Hz). Some studies indicate that strongest EEG power modulations are elicited when the stimulation source is positioned in the center of the visual field and directly fixated [1, 9]. However, it is of particular importance for real-world applications to explore protocols characterized by (1) high user comfort (e.g., by using less perceptible rhythmic stimulation) and (2) feasibility; especially when aiming to integrate the stimulation in everyday life environments (e.g., in a car interior [3]) as well as their respective processes of action (e.g., by using a protocol which does not require direct fixation on the light source, c.f., [7, 8]). Therefore, we investigated topographical modulations (time domain) by measuring ERPs and modulations of oscillatory power (frequency domain) for the four rhythmic light conditions: (1) perceptible FM stimulation with amplitudes of the flickering intensity above a previously estimated individual threshold and (2) non-perceptible FM stimulation with amplitudes below the individual threshold with either (a) direct fixation on the stimulation source (overt attention) or (b) fixation on a crosshair presented 10 cm below the light source (covert attention) in each stimulation condition.

2 Methods

2.1 Participants

EEG data from 12 participants from the same dataset used in [8] were reanalyzed (ten men, mean age of 26.83, $SD = 3.80$). Participants were screened to have normal or corrected-to-normal vision and a visual acuity above 0.7[1]. Furthermore, they were excluded when reporting neurological deficits, central effective medication, drug consumption, or psychiatric disorders. Participants were informed about risk of epileptic seizure due to the rhythmic visual stimulation and signed an informed consent according to recommendations of the declaration of Helsinki. The study was approved by the ethics committee of the Medical Faculty, University of Tuebingen, Germany.

2.2 Apparatus and Stimuli

As in [8], a white-colored light-emitting diode (LED; 2800 K with a peak at 600 nm, diameter 0.5 cm, Model NSPL500DS, Nichia Corporation) with a homogeneous diffusor covering 1.14° of the visual field was mounted in front of a black screen with 1 m distance to the nasion. A crosshair was positioned 10 cm below the LED as fixation point in the

[1] It was measured via the Freiburg Visual Acuity Test [10].

covert condition covering 5.7° of the visual field. The LED was driven by a close-to-real-time capable industrial PC (10 μs; 16-bit). The stimulation and EEG recordings were synchronized via a parallel port and CANopen interface. The rhythmic stimulation was generated with a Beckhoff Framework programmed by AIOCAS S.a.r.l. using a FM stimulation protocol adapted from [6, 7]:

$$signal = A + FV * sin(2 * \pi * Fc * t + (M * sin(2 * \pi * Fm * t))). \quad (1)$$

A represents the amplitude of the current intensity and was estimated individually to define the perceptibility threshold (IPT). *FV* is the fluctuation of the current intensity span with 0.2 mA, *Fc* the carrier frequency (40 Hz), *Fm* the corresponding modulation frequency (30 Hz), *M* the modulation index ($M = 2$) (2), *t* the time vector. Hence, to entrain brain activity, the LED was driven by FM signals at 10 Hz calculated by the difference of *Fc* and *Fm* (40 Hz–30 Hz)[2].

EEG Data Acquisition. EEG potentials were recorded according to the international 10–20 system from the following 32 positions[3] (actiCAP and BrainAmp, BrainProducts GmbH, Germany). The EEG was grounded to FCz and the left mastoid was used as common reference. The impedance was kept below 20 kΩ at the onset of the experiment. The data was digitized at 1000 Hz, high-pass filtered with a time constant of 10 s, and saved for off-line analysis via the BrainVision Recorder (BrainProducts GmbH, Germany).

2.3 Procedure

Participants were seated in a mock-up vehicle interior in a dark recording chamber. First, a 3 min EEG resting state baseline (eyes open and fixated on a crosshair under a shallowly illuminated static light condition; $M = 20$ cd/m^2) was recorded (cf. [8]).

To investigate perceptibility, we designed stimuli either perceptibly flickering above the individual perceptibility threshold intensity (i.e., IPT + 2 mA; A-IPT) or non-perceptibly below the threshold (i.e., IPT - 2 mA; B-IPT). The threshold intensity was estimated prior to the main session with the method of constant stimuli [11] separately for the overt and covert attention condition using 10 repetitions of 14 stimuli (total of 280) with 10 flickering[4] and four static control stimuli without flickering[5]. To cue the attention-based condition, either an arrow signalizing the participant to focus on the LED (overt condition) or a crosshair (covert condition) was presented 8 s before the stimulation onset. In this pre-session, the stimulus was presented for a maximum of 8 s up to 30 s and participants were asked to decide whether the stimulus was flickering or

[2] Since we used a LED with a linear current-to-luminosity curve for the current range used in the experiment, we prevented additional harmonics in the signal due to the fact that the sinusoidal current variations translate into a non-sinusoidal (distorted) light intensity variation.

[3] Positions: Fp1, Fp2, AFz, F7, F3, Fz, F4, F8, FT9, FC5, FC1, FC2, FC6, FT10, C3, Cz, C4, T7, T8, CP5, CP1, CP2, CP6, TP10, P7, P3, Pz, P4, P8, O1, Oz, O2

[4] Flickering stimuli: 0.5 mA, 1 mA, 2 mA, 3 mA, 4 mA, 5 mA, 6 mA, 7 mA, 8 mA, 9 mA

[5] Static control stimuli: 1 mA, 3 mA, 5 mA, 7 mA

not by button press as soon as possible and within 30 s of the stimulation. Each trial was followed by an inter-stimulus interval (ISI) of 10 s.

In the main session, 252 stimuli were presented in 2 (attention; overt - covert) × 3 (perceptibility; A-IPT – B-IPT – static) conditions with 42 repetitions per condition. The conditions were presented block-wise with seven randomized conditions as trials within each block (ISI of 30 s) and six repetitions of the condition within each trial (ISI of 8 s). The attention-based condition was cued 2 s (either with the crosshair or arrow) followed by an 8 s stimulation interval. We Latin-square counterbalanced the order of the conditions within a block with the constraint that the attention-based conditions are (1) alternated and b) equally balanced and pseudo-randomized among participants regarding their order and starting condition. In total, each run lasted 108 s with a break of 30 s afterwards. Each block was followed by a 2 min break. Figure 1 provides an overview of the procedure of the main session.

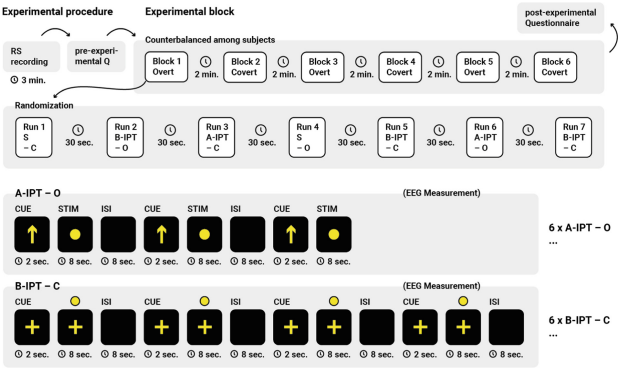

Fig. 1. Experimental procedure of the main session. *RS*: resting state, *Q*: questionnaire; *STIM*: stimulation; *CUE:* cue before the stimulation signaling the attention-based condition; *ISI*: inter-stimulus interval, *S*: static condition, *A-IPT*: above the individual threshold condition, *B-IPT*: below the individual threshold condition; *C*: covert; *O*: overt.

2.4 Data Analysis

EEG Pre-processing. EEG signals were de-trended, zero-padded, and re-referenced to mathematically linked mastoids [12]. We excluded five EEG channels (FT9, FT10, T7, T8, and CP1) from analysis due to artifact contamination. All EEG signals were filtered with a first order zero-phase lag finite impulse response (FIR) filter using a narrow frequency band of 0.5 to 22 Hz for the ERPs and a band-pass filter between 0.5 to 40 Hz for the oscillatory power analysis. The continuous EEG signals were segmented separately for the four conditions with a time window of (1) [−200 to 600 ms] for the ERPs, and 2) [2000 to 6000 ms] for the oscillatory power analysis. Segments containing a maximum deviation above 200 μV in any of the frontal EEG channels (Fp1, Fp2) were rejected. We performed an independent component analysis (ICA) using the logistic infomax algorithm [13] to remove further ocular movement, cardiac, and muscular artifacts via

visual inspection of the topography, time course, and power spectral intensity of the components [14, 15]. Furthermore, the resting state EEG data later used for normalization from each participant was pre-processed as described above for the oscillatory power analysis and divided into non-overlapping epochs of 2 s.

ERP Analysis. For the ERP analysis in the time domain, EEG segments were baseline corrected by subtracting the mean amplitude of a 200 ms time interval before stimulation onset. Signals were then averaged over trials, occipital electrodes (O1, O2), and participants to calculate the grand averages of the ERPs for each condition (see Fig. 2A). To study the topographical changes of the ERPs, three components were statistically evaluated based on [16] (see Fig. 2B and 2C): the (1) P90 [75 to 145 ms], (2) N180 [170 to 245 ms], and (3) P300 [280 to 400 ms]. We used a cluster-based non-parametric randomization approach with multiple comparisons correction [17, 18]. A multiple dependent sample *t*-test on the level of individual electrodes was conducted on the ERP components of the comparisons (1) covert vs. overt condition for A-IPT and B-IPT and (2) A-IPT vs. B-IPT for covert and overt [cf., 19]. Hence, *t*-values exceeding the a priori threshold of $p < .05$ (uncorrected) were spatially clustered based on neighboring electrodes. The cluster level statistics were defined as the sum of *t*-values within each cluster. We corrected for multiple comparisons by calculating the 95th percentile (two-tailed) of the maximum values of summed t-values estimated from an empirical reference distribution. *t*-values exceeding this threshold were, thus, considered as significant at $p < .05$ (corrected). Reference distribution of maximum values was obtained by means of a permutation test (1000 permutations).

Oscillatory Power Analysis. For the calculation of power, we defined regions of interest (ROIs): frontal (F3, Fz, and F4), parietal (P3, Pz, and P4), and occipital electrodes (O1, Oz, and O2). We calculated the power spectra (2–35 Hz) of (1) the resting state and (2) stimulation conditions per ROI for each participant via the fast Fourier transformation (FFT). For the statistical analysis, power was transformed to a dB scale, normalized per condition with the resting state, and binned to frequency bands of interest with alpha (8 to 12 Hz) and beta (18 to 22 Hz) as the first harmonic response. We used a within-subject design with two factors perceptibility (A-IPT and B-IPT) and attention (overt and covert) with non-parametric Friedman's *Q*-tests to statistically analyze the oscillatory power. Subjects revealing extreme reactions to the stimulation were identified as outliers by $M + -2 * SD$ and excluded (one participant in the beta band power). Significant differences between conditions were further analyzed with non-parametric, FDR corrected post-hoc Wilcoxon signed rank tests. Data analyses were performed with custom written scripts in MATLAB® and python™.

3 Results

ERP Results. We observed strongest deflection of the components in electrodes overlying occipital regions in the overt attention condition especially during perceptible stimulation (Fig. 2 A). Comparing the spatio-temporal dynamics of the attention-based conditions (Fig. 2 B), there were reduced positive deflections in electrodes overlying

parieto-occipital regions in the P90 and P300 and increased negative deflection in the N180 during the B-IPT stimulation in the covert (fixation 11.3 deg below the LED) compared to the overt condition (fixation on the LED; upper row). Interestingly, the P300 was enhanced in electrodes overlying the frontal regions in the covert condition under non-perceptible (B-IPT) stimulation. During A-IPT stimulation, reduced positive deflections in electrodes overlying parieto-occipital regions were observable only in early and late components (i.e., P90, P300; lower row). Comparing the perceptibility conditions, significant differences between perceptible (A-IPT) and non-perceptible (B-IPT) stimulations were already present in early components during covert attention (Fig. 2 C, upper row, left). The P90 and P300 were significantly reduced, whereas the N180 was enhanced in electrodes overlying fronto-central regions for the B-IPT (negativity in Fig. 2 C, upper row, due to the contrast non-perceptible vs. perceptible). Further, we found stronger negative deflections in the N180 for the perceptible (A-IPT) stimulation in electrodes overlying the parieto-occipital regions for the covert (positivity in Fig. 2 C, upper row, middle) and overt condition (Fig. 2 C, lower row, middle).

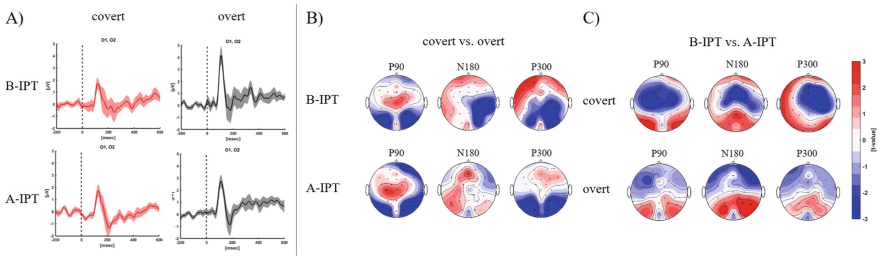

Fig. 2. A) Grand averages of the ERPs in electrodes overlying the occipital regions (O1, O2) for the four conditions. Shades represent the standard error (±SE) of the mean. B) and C) *t*-value topography differences of the P90 (left), N180 (middle), and P300 (right). Electrode clusters showing significant differences in the non-parametric randomization test are indicated by filled black circles. *B-IPT*: below the individual threshold condition; *A-IPT*: above the individual threshold condition.

Oscillatory Entrainment Results. Oscillatory entrainment in the alpha and beta band frequency did not differ between the perceptibility conditions in electrodes over occipital, frontal, and parietal regions. We observed similar power entrainment not only in the overt but also covert attention condition. There was only a significant difference in electrodes overlying occipital regions, $\chi(3) = 2.692$, $p = .021$, between the attention conditions in the non-perceptible stimulation with increased beta band power for the covert condition, $p = .014$ (FDR corrected).

4 Discussion

We observe similar oscillatory power modulations for the four stimulation protocols. In line with [9], we found increased oscillatory power in the first harmonic response

(beta band power) in electrodes overlying occipital regions for the covert compared to the overt condition during non-perceptible stimulation. This finding might be especially interesting for BCI applications [20].

Regarding the ERP results, early exogenous and lately induced ERPs (likely representing the P300 complex [21]) were elicited (cf. [16, 22]). While early components (predominantly located in the primary visual cortex due to the retinotopic activation) indicate processing of psychophysical stimulus features (e.g., contrast, motion, and color [23, 24]), the later represent rather cognitive information processing.

In line with [25–27], we found a clear attention effect reflected in enlarged positive deflections when the stimulation source was overtly attended compared to the covert attention condition. This phenomenon is suggested to reflect attention-related sensory gain control mechanisms in the extrastriate visual cortex associated with enhanced SNR of visual inputs and, thus, improved acuity of visual perception within the spotlight of attention [25–27]. In addition to the reduced P300 deflection in electrodes overlying the centro-parietal/occipital cortex, we observed enhanced frontal P300 deflections for the non-perceptible unattended stimulation. It might point to attentional mechanisms and attempts to identify whether the stimulus is flickering or not. The P300 complex typically associated with the *oddball*-paradigm is sensible to infrequent, deviant stimuli indicating stimulus recognition/discrimination, task-relevant information, and selective attentional processing [21]. It is further associated with working memory capacity and updating processes [21]. Contrary to [27], the N180 deflection was enlarged in electrodes overlying parieto-occipital regions when the non-perceptible stimulation was unattended compared to the overt attention condition. The N180 complex (originally N135 but slightly shifted due to the rhythmic light stimulation [16]) activates magnocellular pathways of the visual system associated with processing of luminance, non-color, and motion related information [22–24]. A possible explanation could be cortical hyperexcitation due to reduced inhibitory activity of cortical pyramidal cells during non-perceptible and unattended stimulation [28].

5 Conclusion

Our findings indicate entrainment effects represented in both ERPs and power even for a non-perceptible stimulation and without directly fixating on the light source. This non-invasive stimulation method shows strong potential for naturalistic applications to enhance neuronal activity and cognitive processes. Especially for safety-critical situations, the possibility to enhance alertness, concentration, or/and performance is appealing. However, a complete understanding of rhythmic light stimulation is a precondition for application in traffic and other safety relevant areas. The work contributes to understanding and potential use of non-invasive and non-perceptible rhythmic light stimulation.

References

1. Herrmann, C.S.: Human EEG responses to 1-100 Hz flicker: resonance phenomena in visual cortex and their potential correlation to cognitive phenomena. Exp. Brain Res. **137**(3–4), 346–353 (2001)

2. Vialatte, F.-B., Maurice, M., Dauwels, J., et al.: Steady-state visually evoked potentials: focus on essential paradigms and future perspectives. Prog. Neurobiol. **90**(4), 418–438 (2010)
3. Fan, X., Bi, L., Teng, T., et al.: A brain-computer interface-based vehicle destination selection system using P300 and SSVEP signals. IEEE Trans. Intell. Transport. Syst. **16**(1), 274–283 (2015)
4. Notbohm, A., Herrmann, C.S.: Flicker regularity is crucial for entrainment of alpha oscillations. Front. Hum. Neurosci. **10**, 503 (2016)
5. Notbohm, A., Kurths, J., Herrmann, C.S.: Modification of brain oscillations via rhythmic light stimulation provides evidence for entrainment but not for superposition of event-related responses. Front. Hum. Neurosci. **10**, 10 (2016)
6. Dreyer, A.M., Herrmann, C.S.: Frequency-modulated steady-state visual evoked potentials: a new stimulation method for brain-computer interfaces. J. Neurosci. Methods **241**, 1–9 (2015)
7. Dreyer, A.M., Herrmann, C.S., Rieger, J.W.: Tradeoff between user experience and BCI classification accuracy with frequency modulated steady-state visual evoked potentials. Front. Hum. Neurosci. **11**, 391 (2017)
8. Lingelbach, K., Dreyer, A.M., Schöllhorn, I., et al.: Brain oscillation entrainment by perceptible and non-perceptible rhythmic light stimulation. Front. Neuroergon. **2,** 9 (2021)
9. Ordikhani-Seyedlar, M., Sorensen, H.B.D., Kjaer, T.W., et al.: SSVEP-modulation by covert and overt attention: novel features for BCI in attention neuro-rehabilitation. In: Annual International Conference of the IEEE Engineering in Medicine and Biology Society, pp. 5462–5465 (2014)
10. Bach, M.: The Freiburg Visual Acuity test–automatic measurement of visual acuity. Optom. Vis. Sci. **73**(1), 49–53 (1996)
11. Eisen-Enosh, A., Farah, N., Burgansky-Eliash, Z., et al.: Evaluation of critical flicker-fusion frequency measurement methods for the investigation of visual temporal resolution. Sci. Rep. **7**(1), 15621 (2017)
12. Nunez, P.L., Srinivasan, R.: Electric Fields of the Brain. Oxford University Press, Oxford (2006)
13. Delorme, A., Makeig, S.: EEGLAB: an open source toolbox for analysis of single-trial EEG dynamics including independent component analysis. J. Neurosci. Methods **134**(1), 9–21 (2004)
14. Chaumon, M., Bishop, D.V.M., Busch, N.A.: A practical guide to the selection of independent components of the electroencephalogram for artifact correction. J. Neurosci. Methods **250**, 47–63 (2015)
15. Hipp, J.F., Siegel, M.: Dissociating neuronal gamma-band activity from cranial and ocular muscle activity in EEG. Front. Hum. Neurosci. **7**, 338 (2013)
16. Gaume, A., Vialatte, F., Dreyfus, G.: Transient brain activity explains the spectral content of steady-state visual evoked potentials. In: Annual International Conference of the IEEE Engineering in Medicine and Biology Society, pp. 688–69 (2014)
17. Maris, E., Oostenveld, R.: Nonparametric statistical testing of EEG- and MEG-data. J. Neurosci. Methods **164**(1), 177–190 (2007)
18. Oostenveld, R., Fries, P., Maris, E., et al.: FieldTrip: open source software for advanced analysis of MEG, EEG, and invasive electrophysiological data. Comput. Intell. Neurosci. **2011**, (2011)
19. Vukelić, M., Gharabaghi, A.: Oscillatory entrainment of the motor cortical network during motor imagery is modulated by the feedback modality. Neuroimage **111**, 1–11 (2015)
20. Müller-Putz, G.R., Scherer, R., Brauneis, C., et al.: Steady-state visual evoked potential (SSVEP)-based communication: impact of harmonic frequency components. J. Neural Eng. **2**(4), 123–130 (2005)
21. Polich, J.: P300 as a clinical assay: rationale, evaluation, and findings. Int. J. Psychophysiol. **38**(1), 3–19 (2000)

22. Odom, J.V., Bach, M., Brigell, M., et al.: ISCEV standard for clinical visual evoked potentials: (2016 update). Doc. Ophthalmol. **133**(1), 1–9 (2016)
23. Souza, G.S., Gomes, B.D., Lacerda, E.M.C.B., et al.: Amplitude of the transient visual evoked potential (tVEP) as a function of achromatic and chromatic contrast: contribution of different visual pathways. Vis. Neurosci. **25**(3), 317–325 (2008)
24. Ellemberg, D., Hammarrenger, B., Lepore, F., et al.: Contrast dependency of VEPs as a function of spatial frequency: the parvocellular and magnocellular contributions to human VEPs. Spat. Vis. **15**(1), 99–111 (2001)
25. Hillyard, S.A., Vogel, E.K., Luck, S.J.: Sensory gain control (amplification) as a mechanism of selective attention: electrophysiological and neuroimaging evidence. Philos. Trans. R. Soc. Lond. B Biol. Sci. **353**(1373), 1257–1270 (1998)
26. Handy, T.C., Khoe, W.: Attention and sensory gain control: a peripheral visual process? J. Cogn. Neurosci. **17**(12), 1936–1949 (2005)
27. Müller, M.M., Hillyard, S.: Concurrent recording of steady-state and transient event-related potentials as indices of visual-spatial selective attention. Clin. Neurophysiol. **111**(9), 1544–1552 (2000)
28. Fong, C.Y., Law, W.H.C., Braithwaite, J.J., et al.: Differences in early and late pattern-onset visual-evoked potentials between self- reported migraineurs and controls. Neuroimage Clin. **25**, (2020)